Spring 2019

Charged Particle Filter for Entrance of IMAP-Lo

Daniel Abel

Charged Particle Filter for Entrance of IMAP-Lo

By:

Daniel Abel

May 15, 2019

Department of Engineering Physics

Table of Contents

Defined Terms

IMAP – Interstellar Mapping and Acceleration Probe

IBEX – Interstellar Boundary Explorer

SIMION – Simulation program used for this study

IM – Interstellar Medium

ESA – Electrostatic Analyzer

TOF – Time of Flight System

FOV – Field of View

Abstract

The Interstellar Mapping and Acceleration Probe's (IMAP) mission is to investigate "the acceleration of energetic (neutral) particles and the interaction of the solar wind with the interstellar medium" (1). IMAP-Lo is one of ten IMAP instruments and one of three neutral atom instruments working together. It will gather information from 10-1,000eV neutral atoms that come from the interstellar boundary. An important requirement for neutral atom instruments is that they effectively reject the more abundant electrons and ions from entering. The research and design problem presented here consists of a trade study between the original rejection entrance design of IBEX-Lo and a new deflection entrance design. This study was conducted using a particle flight simulation program called SIMION to accurately test the behavior of different charged particle distributions for various design geometries of the IMAP-Lo entrance system. The results show that the deflection design out-performs the original rejection design and completely eliminates the adverse "ion gun" effect that the original design produced. However, for the deflection design to be more effective, an extension of the outer wall is necessary to block incoming positive ions that have an angle of approach close to the outer negative electrode. With the addition of the outer wall extension, the deflection design uses lower voltages to prevent more of the same charged particles than the rejection design while also completely eliminating the harmful "ion gun" effect.

Introduction

The interstellar medium (IM) is defined as the material that lies between star systems inside galaxies. This material is primarily composed of hydrogen and helium, with trace amounts of heavier elements. The Sun moves through the interstellar medium with a speed of approximately 70,000 km/hr while also producing solar wind containing charged particles (Figure 1). The solar wind travels radially outwards with the pressure dropping over distance. Since the solar wind consists of charged particles, it carries with it magnetic and electric fields outwards, away from the Sun. The area where the solar wind pressure is similar to the IM impact pressure is called the heliopause. Here, the fields carried by the Solar wind are separated from the electric and magnetic fields produced in the interstellar medium. This causes the charged particles in the

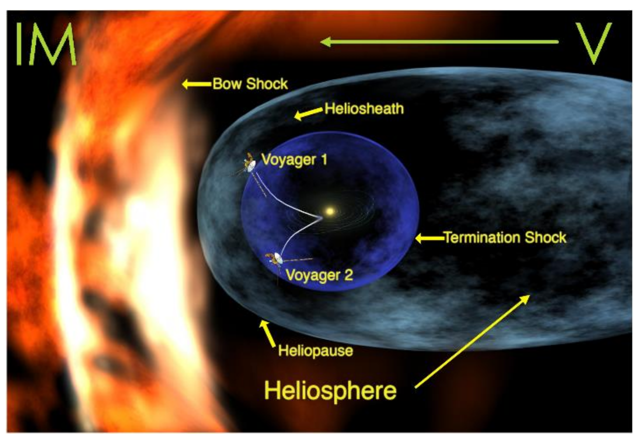

Figure 1: Sun moving through the interstellar medium [Zell, Holly. 2015]

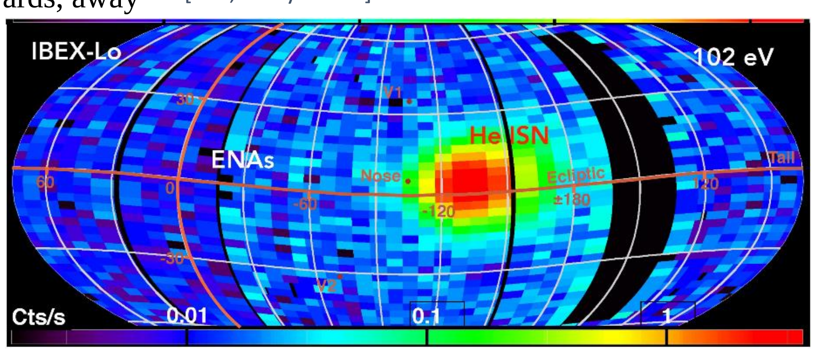

Figure 2: An ENA map of the heliopause created by IBEX-Lo

IM to be deflected away from the Sun. However, there are also neutral particles in the IM and more are produced in the heliospheric boundary region that will not be affected by these field interactions and they can move toward the Sun, only deflected by gravitational effects. IMAP is trying to measure these energetic neutral atoms (ENAs) from the IM and the boundary region. IMAP-Lo's main goal is to detect these ENAs at energies ranging from 10eV-1,000eV. The spacecraft will rotate on an axis perpendicular to the instrument FOV. As it rotates, the IMAP sensors will collect neutrals from the part of the sky they are facing, scanning a circle in the sky. After half a year IMAP-Lo will create a complete sky map of ENAs at different energies (similar to the one from IBEX-Lo shown in Figure 2).

IMAP-Lo Instrument Description

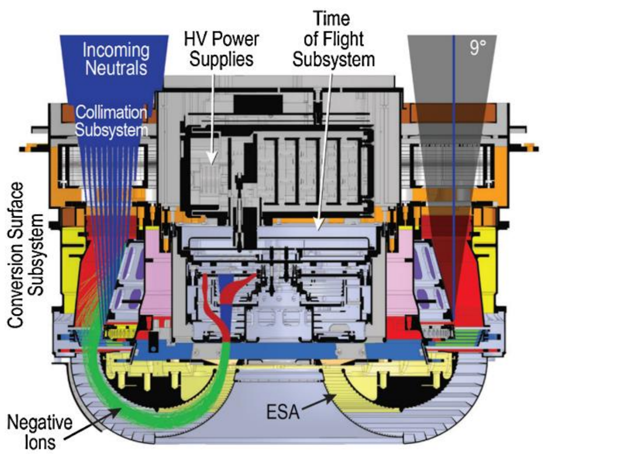

Figure 3: A center-cut view of the IMAP-Lo instrument with neutral particle paths drawn from entrance to TOF system [McComas et al., 2018]

The original instrument that was sent out to observe low energy ENAs was IBEX-Lo and IMAP-Lo will have a similar design (Figure 3). The incoming neutrals enter through a collimator that filters out certain directions. These ENAs will then impact a carbon-coated conversion surface, where they are converted to negative ions. Then the ions will be directed through an electrostatic analyzer (ESA). With a given voltage across the ESA, only ions with desired energies will be able to make it through the 180° curve. Particles with energies outside of the desired range will impact the serrations and not make it around the curve. The ions that do make it through the ESA will be accelerated by a positive 16 kV post-acceleration voltage and then enter the time-of-flight system. This system measures the velocity of the ions by measuring the difference in impact times of individual particles between two thin foils and a stop detector. By determining the energy (from the post-acceleration voltage and ESA voltage) and velocity, the mass of these ions can be obtained. Once the mass is calculated, the species can be determined and the composition of the interstellar medium can be measured [Fuselier. 2009]. Since there is such a low rate of incoming neutrals, it is important to reduce any background as much as possible. There is a much higher flux of energetic charged particles in the instrument's environment than neutral atoms, and it is very important to filter out as many of these as possible, hence the purpose of this study.

Design Challenge for the IMAP-Lo Entrance System

The challenge for this study is that the IMAP-Lo instrument will be exposed to a very large number of charged particles in the environment of the spacecraft location. This is mostly caused by the solar wind, since the instrument will be within the bounds of the solar system. If these charged particles were to enter IMAP-Lo, they would cause a lot of background compared to the low rate of neutrals the instrument is expected to receive. The entrance system helps to keep these charged particles out by putting voltages on the electrodes and/or the collimator located at the entrance. These voltages can alter the path of incoming charged particles so that they do not impact the conversion surface, where they inject erroneous signals into the data.

The hypothesis for this study is that the new deflection voltage design (Figure 5) will function similarly or better than the original rejection design (Figure 4). It will ideally use a lower voltage to deflect more electrons and positively charged ions away from the conversion surface while also eliminating the "ion gun" effect caused by having the collimator set to a positive voltage in the original IBEX design. The "ion gun" effect is caused first by the outgassing of particles from surfaces inside the instrument once exposed to the vacuum of space. These particles leave the surface and wander around the instrument. Eventually they can end up right behind the collimator (shown in Figure 4) and become positively charged by incoming high energy particles and UV radiation. Once positively charged these outgassed particles will be accelerated towards the conversion surface due to the collimator being set to a positive potential. As a consequence, they can impact the conversion surface and increase the background in the data.

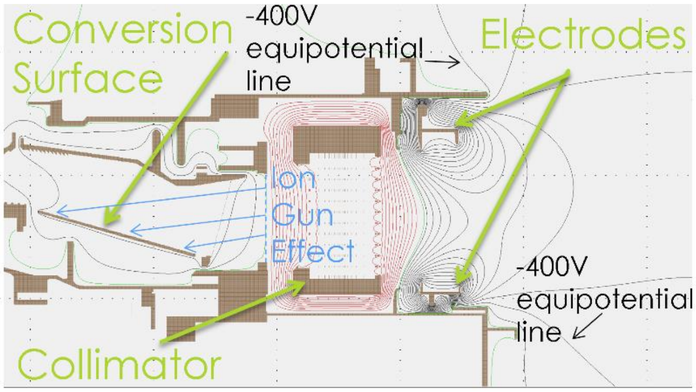

Figure 4: The original rejection voltage design showing the "ion gun" effect and equipotential lines.

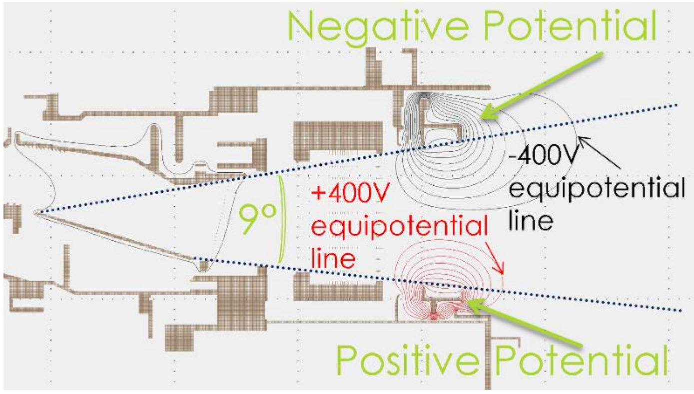

Figure 5: The new deflection voltage design with resulting equipotential lines and elimination of the "ion gun" effect

The new deflection design will instead set the collimator to ground. This will eliminate the "ion gun" effect because there is no acceleration of the outgassed particles anymore. The new design will also set the outer electrode to a negative potential and the inner electrode to a positive potential. By doing this, a dipole field is created which has a much more contained potential configuration facing the vacuum of space compared to the previous negative monopole potential in the rejection design. This new voltage configuration should affect nearby instruments, which are also sensitive to electric fields, much less than the rejection design.

Design Evaluation Method

The first step in this trade study was to simulate the original rejection design versus the new deflection design, using the SIMION program. This program is used to simulate particle paths and the influence electric potentials have on those trajectories. Geometries in this program define the shape of physical objects that these particles can interact with and impact during flight. First, a geometry is chosen for simulation and is tested for different voltage steps on the electrodes and collimator (depending on design). Once a geometry and voltages are chosen, a particle population is determined. This population has starting positions and energies (100eV-2,000eV) determined from the birth of the particle. These starting positions can be seen in Figure 6 with each color representing a different range of angles. After a particle has left its starting point the geometry and electric fields, produced by the voltages, determine its path through the instrument. Once all voltage and energy steps have been simulated for a design, another design is chosen and the process is repeated.

The SIMION program can accurately determine electric field strengths and calculate particle trajectories through these electric fields. It is very important to be able to find these effects on particle trajectories so that the effectiveness of different designs can be tested. However, this program is only accurate to a max of $^{1}/_{10}{}^{th}$ of a millimeter and some features, like the honeycomb design of the collimator, cannot properly be modeled. Since these simulations are being run with a 2D cut of the configuration, the honeycomb design does not need to be modeled. Similar designs are used in the program to simulate how the actual design should function in actual testing. The FOV must also stay at 9° and nothing is allowed to enter this region. This allows for a maximum viewing angle of neutrals to enter the collimator and impact the conversion surface.

Optimization of the New Deflection Design

In Figures 6 and 7, the different colors represent different angular distributions to be able to determine the direction of the ions hitting the conversion surface. For the deflection design with the original geometry, it is shown that the majority of the ions that were hitting the conversion surface were colored red and coming from angles close to 90° from the entrance and from the outer direction (as shown in Figure 6). This is due to the outer electrode being set to a negative potential and curving these red ions directly toward the conversion surface.

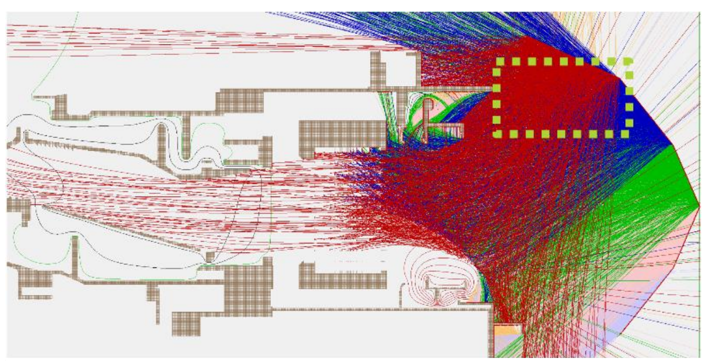

Figure 6: Positive ion trajectories without the outer shield wall extension

The outer shield wall was extended a total of 47.8mm (Figure 7) farther out than the original design. The wall stays outside of the FOV and does not impact ENA approach angles. IBEX-Lo originally had a space constraint and could not implement this wall extension. However, IMAP-Lo does not have this restriction.

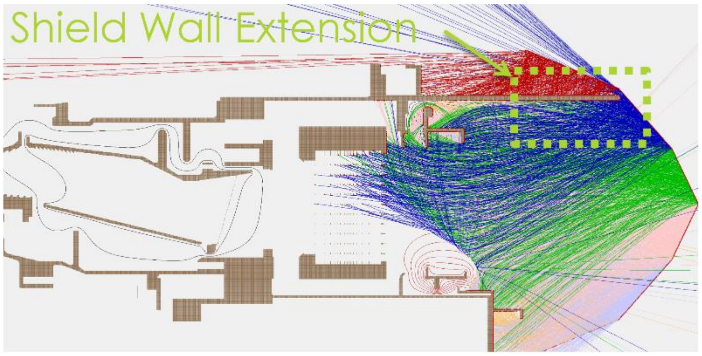

Figure 7: This shows the outer wall extension blocking many of the angular distribution on ions that were previously impacting the conversion surface

The outer wall extension (Figure 7) clearly blocks out many of the incoming positive ions that previously were impacting the conversion surface. This simple extension can reduce the necessary voltage needed to deflect ions while also eliminating all of the ions coming from the red direction. The addition of a shield wall physically blocked an average of 51.58% more positive ions (from 1,000ev – 2,000eV).

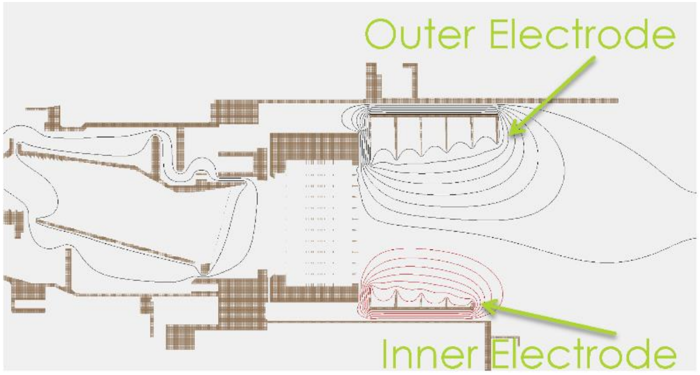

Figure 8: The figure above shows the 6-prong (66.8mm) outer electrode design

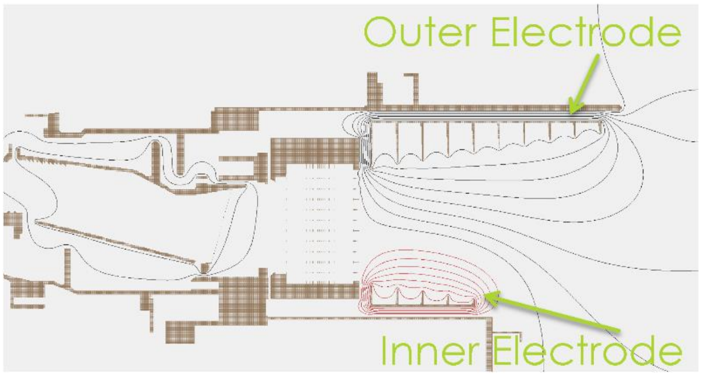

Figure 9: The figure above shows the 10-prong (85.4mm) outer electrode design

In the next step, the inner electrode was redesigned to utilize more space outside of the 9° FOV. Three outer electrode designs (6-prong (48mm), 8-prong (66.8mm), and 10-prong (85.4mm)) were tested to see if any significant difference in deflection results could be determined. Figure 8 shows the 6-prong outer electrode design. Figure 9 shows the 10-prong outer electrode design and shows the extent of unobstructed FOV of the instrument. The inner electrode was held at a constant length of 38.6mm during the testing for these three designs because the FOV did not allow for more extension or variation. In all designs, a minimum spacing of 3mm (1kv/1mm) was used between the electrodes and any flat surface nearby to prevent strong potential gradients and discharges.

Simulation Results

In the following, we compile the simulation results graphically to compare the different evolutions of the design. In all graphs we compare ions ranging from 1,000eV – 2,000eV, except in Figure 11, which shows electrons. In Figures 10 and 11, the solid line refers to deflection design while the dashed line represents the original rejection design. In Figures 12 and 13, the solid line represents the more effective design in the comparison while the dashed line refers to the less effective design. In all of the figures below, the red coloring refers to the 2,000eV particles, the green coloring represents the 1,500eV particles, and the blue coloring refers to the 1,000eV particles flown during these comparisons. The x-axis shows different electrode voltages while the y-axis shows the percentage of ions that impacted the conversion surface. The purpose of these graphs is to visually compare two different designs and see which one is more effective at preventing particles from hitting the surface.

Figures 10 and 11 compare the original rejection voltage design to the new deflection voltage design without changing the geometry of the instrument as shown in Figures 4 and 5. Figure 11 shows the deflection design out-performing the rejection design when preventing electrons from impacting the conversion surface. However, the rejection design still outperforms the deflection design when using the same geometry to prevent ions. This is due to the negative electrode curving ions coming from ~90° from the entrance plane directly towards the conversion surface. An extension of the outer wall eliminates this angle of approach and many of those ions that were previously entering the instrument.

Figure 12 demonstrates the effectiveness of the outer wall extension compared to the same voltage design without the extension. This graph is important because it shows a clear improvement over the design without the wall extension. Lastly, Figure 13 compares the effectiveness of the 6-prong and 10-prong outer deflection electrode preventing ions from reaching the conversion surface more effectively. It shows the 10-prong electrode slightly out-performing the 6-prong electrode while utilizing more space outside the FOV.

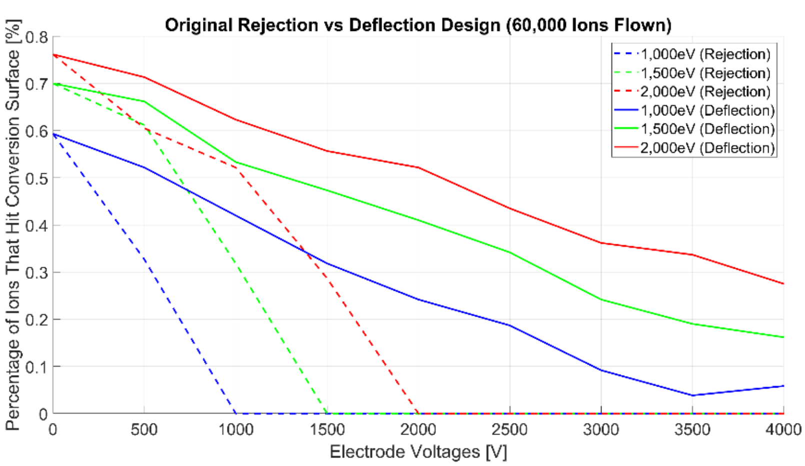

Figure 10: The graph to the left compares the original rejection design versus the new deflection design over a range of voltages. The particles flown here are positive ions ranging from 1,000eV to 2,000eV. The total particle count in these tests is 60,000 ions.

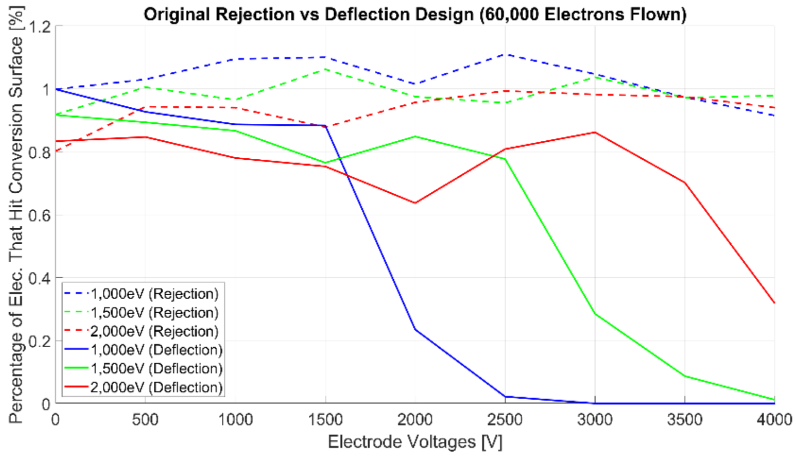

Figure 11: The graph to the left compares the original rejection design versus the new deflection design over a range of voltages. The particles flown here are electrons ranging from 1,000eV to 2,000eV. The total particle count in these tests is 60,000 electrons. Based on this graph the deflection design blocked, on average, 44.45% more electrons from impacting the conversion surface.

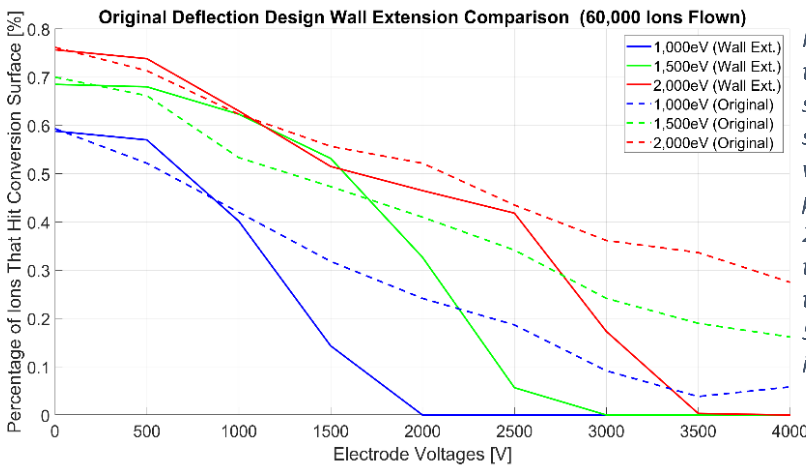

Figure 12: The graph to the left compares the new deflection design versus the same design but with the 47.8mm outer shield wall extension over a range of voltages. The particles flown here are positive ions ranging from 1,000eV to 2,000eV. The total particle count in these tests is 60,000 ions. Based on this graph the wall extension blocked, on average, 51.58% more positive ions from impacting the conversion surface.

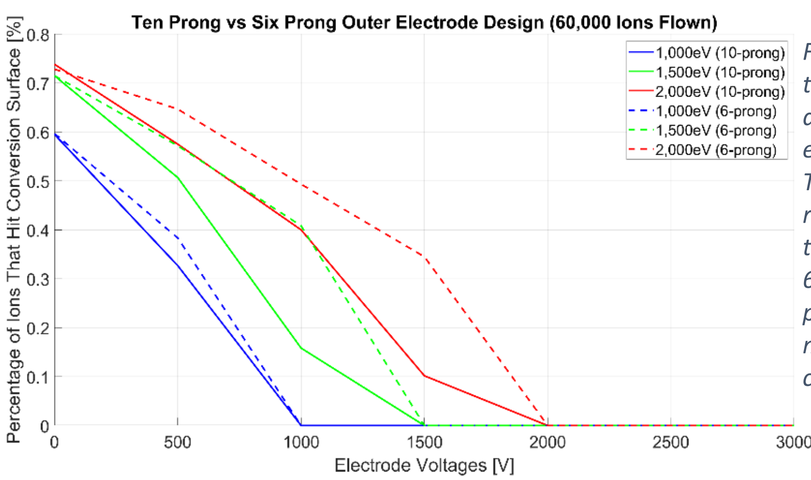

Figure 13: The graph to the left compares the ten-prong (85.4mm) outer electrode design versus six-prong (48mm) outer electrode design over a range of voltages. The particles flown here are positive ions ranging from 1,000eV to 2,000eV. The total particle count in these tests is 60,000 ions. Based on this graph the ten-prong design blocked, on average, 6.74% more positive ions from impacting the conversion surface.

Analysis of the Results and Discussion

To quantitatively assess the results, the equation $r = 1 - \left(\frac{n_1}{n_2}\right)$ was used. r is the ratio of effectiveness between two designs. n_1 is the number of particles that hit the conversion surface from the more effective design while n_2 is from the less effective design. The ratio (r) was obtained for each voltage step was gained and then averaged for a single particle energy. The ratios for all three energies for each design were then averaged to obtain the final ratio. All percentages are based on ion populations with energies ranging from 1,000ev – 2,000eV.

The purpose of this study is to determine the effectiveness of both the rejection and deflection entrance designs for IMAP-Lo. Once a more effective design is determined, it is then optimized to prevent as many charged particles from impacting the conversion surface as possible. Through simulations of different designs and electrode lengths using the SIMION program, it is determined that the deflection design blocked, on average r = 41.45%* more electrons than the previous rejection design. It also set the collimator to ground, completely eliminating the harmful "ion gun" effect while also reducing the field line strength farther away from the instrument due to its dipole electric field. A shield wall extension of 47.8mm blocks an extra r = 51.58%* more positive ions while using the same voltages and overall design. The ten-prong (85.4mm) outer electrode blocked, on average, r = 6.74%* more positive ions versus the six-prong (48mm) design. In conclusion, the deflection design (more specifically the 85.4mm electrode design) should be strongly considered for the design of IMAP-Lo's entrance moving forward. (* - These percentages are based on results from 1,000eV – 2,000eV)

Conclusions

By changing the configuration of the instrument entrance system from the previous rejection design to a deflection design, we completely eliminate the "ion gun" effect. In the new design positive ions produced from outgassing materials are no longer accelerated towards the conversion surface. Now that the collimator is grounded the original ceramic insulators can also be eliminated, saving materials and space, and reducing risk of failure. By setting the outer electrode to a negative potential and the inner electrode to a positive potential, a dipole field is produced. This dipole has a more contained potential configuration compared to the original monopole field. This design modification reduces the negative effects on surrounding sensitive instruments. The deflection design can prevent 2,000eV ions with ±2kV set to the electrodes. This is a 50% decrease in voltage used compared to what the previous design utilized. 2,000eV ions have an energy that is twice the highest energy range of the instrument. If ions of higher energy need to be eliminated, the electrode voltages can be scaled proportionally.

Future Work

In a future expansion of this work, a larger source population for both positive ions and electrons should be used to reduce error and cover more incoming angles. Source populations should be moved outside the influence of the electric fields to create a more accurate simulation of their approach. A logarithmic energy scale should be used instead of a linear scale to reduce redundancy in simulations. A "wrap around" design of the shield wall at the front end of the inner and outer electrodes should be tested to reduce the reach of electric field lines even further.

Works cited

1. Zell, Holly. "The Heliosphere." *NASA*, NASA, 2 Mar. 2015, www.nasa.gov/mission_pages/sunearth/science/Heliosphere.html.
2. McComas, D. J., et al. "Interstellar Mapping and Acceleration Probe (IMAP): A New NASA Mission." *SpringerLink*, Springer Netherlands, 22 Oct. 2018, link.springer.com/article/10.1007%2Fs11214-018-0550-1.
3. Fuselier, S. A., A. G. Ghielmetti, E. Hertzberg, A. S. Moore, D. Isaac, J. W. Hamilton, C. Tillier, E. Moebius, M. S. Granoff, D. Heirtzler, B. King, H. Kucharek, S. Longworth, J. Nolin, S. Turco, S. Ellis, J. Googins, F. Kudirka, J. Tyler, M. Vosbury, G. Clark, M. O'Neal, P. Wurz, J. Scheer, L. Saul, D. Piazza, P. Bochsler, M. Wieser, C. Schlemm, D. J. McComas, J. Scherrer, S. Pope, H. O. Funsten, D. Chornay, J. Lobell, T. E. Moore, P. Rosmarynowski, T. Friedmann, R. J. Nemanich, IBEX-Lo Sensor, Space Sci. Rev., 146, 117, 10.1007/s11214-009-9495-8, 2009.